

Compact Motors and Drives for Electric Vehicles

UDK 621.313.392:629
IFAC IA 5.6.2

Preliminary communication

Due to their high efficiency, brushless PM rotor motors are very suitable for vehicle drive application. This paper presents experimental results of a newly developed technique in brushless motors. It is suitable for both square current and DSP-controlled sinusoidal current drives. The experimental result of such systems is described. The drive systems, including the inverter, the motor and the controlling software have been developed by the authors. Also, popular controlling algorithms have been used, and a common way to initialise them in order to enable to operate with any kind of motors.

Key words: electric vehicles, brushless drives, automotive application, adaptive control, DSP, vector control, neural networks, sliding mode control, simulation

1 INTRODUCTION

In the past 10–15 years, numerous brushless vehicle drives have been developed by the authors for scooters, wheelchairs, golf-cars, bicycles. Vehicle drives for scooters, golf-, and electrical cars are shown in Figure 1 and 2.

The motor structure varies in rotor and stator layout, representing a wide range including inner and outer rotor, surface mounted and internal magnet, radial and axial flux motors, or ironless stators. These drives are 12–36 V/30–200 A battery-voltage systems.

The compact systems include an in-wheel machine with integral electronics, a planetary gear drive

and stop brake (see Figure 3). All of them use Hall-effect position detectors. The motors are fully specialised for the given task.

Table 1 contains benchmark results for the different drive types after a 2000 km test period for each.

As the table shows, brushless (EC and PM synchronous) motors are 25–35 % more effective than DC motors. Our EC motors are of a trapezoidal emf shape and they are driven with square-shaped current, having low torque ripple. At present, square current driven motors seem to be the best solution as battery voltage vehicle drives. They are so simple and robust that sinusoidal-shaped motor drives cannot compete with them in price. As mi-



Fig. 1 Brushless drives: a) a front driven 3-wheeled bike; b) a golf-car



Fig. 2 Electrical car («Bringo») for tourists used on Margaret Island in Budapest

Table 1 Benchmark of different drive types

Application	Motor type	DC voltage V	Battery charge Ah	Trip range km
Golf-car	DC	24	240	70–90
Golf-car	EC	24	240	110–130
Golf-car	PMSM	24	240	110–130
Wheelchair	DC	24	40	25–35
Wheelchair	EC	12	55	25–30

EC – Electronically Commutated DC motor (square current)
 PMSM – Permanent Magnet Synchronous Motor (sinusoidal emf and current)

Microcontrollers become more and more available and cheap, more refined systems can be used in low cost applications. A microcontroller-controlled drive has been designed by the authors for low power electrical vehicles that is shown in Figure 4.

There is a tendency towards using high speed EC motors with internal planetary gear (PG) drive in cars, in order to reduce mass (Figure 3.b). We also implement PG drives of a gear ratio from 3:1 to 11:1. In small power applications where the allowed speed is low, high pole numbers are used (8, 10, 12). In high power applications, where high vehicle speed is aimed, low pole numbers are preferred (4, 6, 8). High power drives, like our golf-car drive, are load-angle controlled as well, in order to increase the torque at the low speed range, and reduce the induced voltage at the high speed range. During normal operation, the commutation instance is set to its theoretical position, for good efficiency.

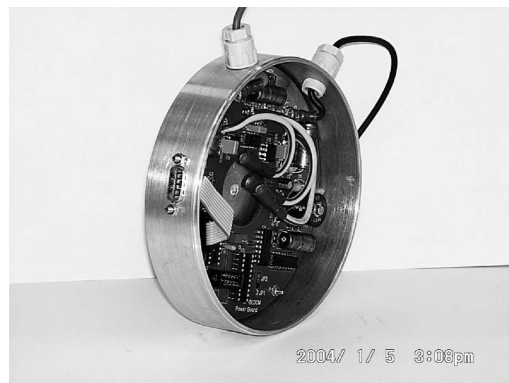


Fig. 4 Electronics of the microcontroller controlled brushless motor drive

2 NEW DEVELOPMENTS

Our newest development is a 72 V/600 A axial field PM motor and power electronics (Figure 5). Its purpose is to drive an electric racing car at a FIA cup.

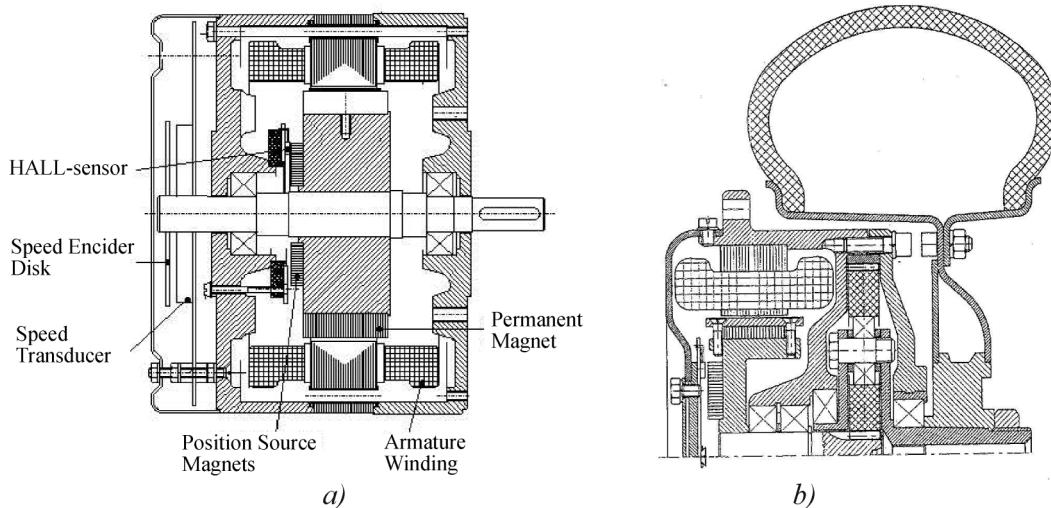


Fig. 3 Brushless motor applications: a) with internal electronics; b) compact in-wheel EC drive for wheelchair

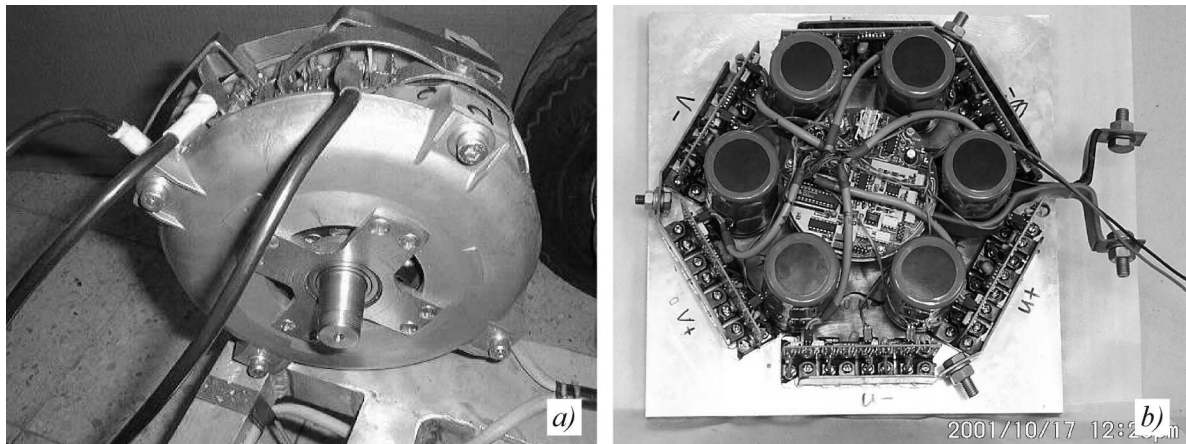


Fig. 5 Our new developments: a) axial field racing motor; b) power electronics for racing motor

The most special goal of the development was to achieve the highest possible power per mass ratio, regarding that pure natural ventilation has been applied. A recuperation of high-efficiency has been another requirement of high priority since a vehicle must do a whole race without recharging the batteries, according to the prescriptions of the championship. Due to the relatively low voltage and high current, we must have to manage the problems in connection with the non-ideal behaviour of the batteries and power rails at high frequencies.

The newly developed power electronics (Figure 5.b) has the following main characteristics: the MOSFET drivers are fully isolated from the control circuit; short circuit protection based on observing the saturation voltage of the power MOSFETS; hardware Hall-effect sensor position decoder realised in a GAL; maximum current limitation inside a PWM cycle; automatic changing between driving and braking mode.

3 NEW APPLICATION DEVELOPMENT METHOD

Application development requires a complex, very long testing and developing procedure for testing a huge number of configurations and control algorithms. Although a final algorithm can only be placed into some marketable hardware, their development is the most comfortable on PC-s.

The use of a DSP system makes it possible to simulate a future control system (even hardware) to analyse its effectiveness. This makes it possible to evaluate numerous configurations and algorithms without any serious reconfiguration of the hardware. Let us show an example for system development with this integrated method.

For the DSP-controlled system, a new, sinusoidal voltage and current motor have been developed.

The realised sinusoidal emf shape with rare-earth magnets has given good experiment results.

Rotor position can be observed either by the means of a position encoder or some position estimation method. A usual way of position sensing is the use of a resolver. This device needs accurate setting and is expensive. A much cheaper solution is the use of low-resolution hall-effect sensors and some algorithm that makes position detection more accurate.

An alternative solution is a DSP-based measuring and controlling device, which estimates the rotor position from the working parameters of the motor. This method is widely applied in servo drives and high power traction applications. Battery powered vehicles may also be driven with such a method. The following part describes this possibility. Moreover, this way of solving the problem may also implement auxiliary sensors, so it is very flexible. Such a high performance digital controller can also be further developed only by re-programming it, e.g. including multiple control loops in a single device, making it space-effective.

4 THE DIRECT FLUX-ESTIMATION METHOD IN POSITION DETECTION

The electrical models can be used for absolute or relative position detection, and they are based on the magnetic asymmetry of the rotor. One source of asymmetry may be the directed rotor flux (this is used in this case); another one may be the varying inductivities in the d and q directions of the rotor reference frame.

$$\begin{bmatrix} u_A \\ u_B \\ u_C \end{bmatrix} = \begin{bmatrix} U_{DC} \cos \theta \\ U_{DC} \cos \left(\theta - \frac{2\pi}{3} \right) \\ -(u_A + u_B) \end{bmatrix}. \quad (1)$$

The theory of this method is well known. The phase currents are measured at two outputs of the voltage source inverter, the algorithm commands the output voltages. Knowing the armature resistance and inductivity, the electric models of the motor will give us the instantaneous pole flux values, from which the rotor position is calculated. The algorithm needs to know the number of control cycles in a π electric cycle length. A simple trick gives good results: The output command signals are analysed by the following speed-computing algorithm.

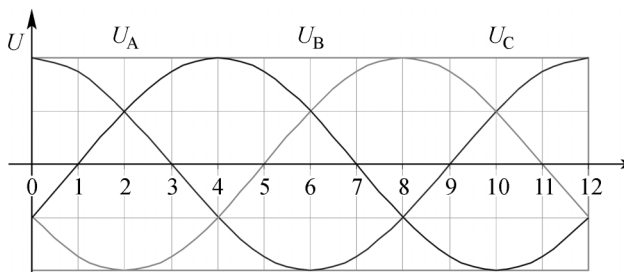


Fig. 6 Segments of the phase voltage command

Table 2 Discrimination rules for 12 position segments of the phase voltage command

Rules	$\lambda, \pi/6$
$u_A > 0 > u_B > u_C$	0...1
$u_A > u_B > 0 > u_C$	1...2
$u_B > u_A > 0 > u_C$	2...3
$u_B > 0 > u_A > u_C$	3...4
$u_B > 0 > u_C > u_A$	4...5
$u_B > u_C > 0 > u_A$	5...6
$u_C > u_B > 0 > u_A$	6...7
$u_C > 0 > u_B > u_A$	7...8
$u_C > 0 > u_A > u_B$	8...9
$u_C > u_A > 0 > u_B$	9...10
$u_A > u_C > 0 > u_B$	10...11
$u_A > 0 > u_C > u_B$	11...12

The Figure 6 and Table 2 show how to get the actual position segment of the phase voltage command vector. The speed computation algorithm counts the control cycles between the changes in position segments. It also generates real shaft rpm as well.

The scheme of the simplified position detector is shown in Figure 7. The main advantage of this method is that it does not require the measurements of any $\frac{di}{dt}$, so the measurement noises are acceptably moderate.

The next step is current controlling, so that the direction of the current vector is related to the estimated rotor position.

5 A SLIDING MODE CURRENT CONTROLLER WITH A CURRENT MODEL IN THE ROTOR COORDINATE SYSTEM

If the ideal behaviour of a system is known and compared to its real behaviour, their difference gives the »unideality« of the real system. This unideality is the sum of external disturbances and internal parameter variations ($\hat{\lambda}$, see Figure 8). Since both factors are disadvantageous for the controllability of the system, both should be eliminated by feeding back and subtracting from the input (u).

In our system, a simple model of the $u-i$ characteristics of the motor is used:

$$i_d = \frac{\Psi_d - |\Psi_{PM}|}{L_d}, \quad i_q = \frac{\Psi_q}{L_q}, \quad (2)$$

where $\Psi_{d,q}$ are the main flux components, and $|\Psi_{PM}|$ is the magnitude of the pole flux linkage.

The only problem with this structure is feedback signal computation. Sliding mode controllers use a relay (signum or hysteresis, two or three level) he-

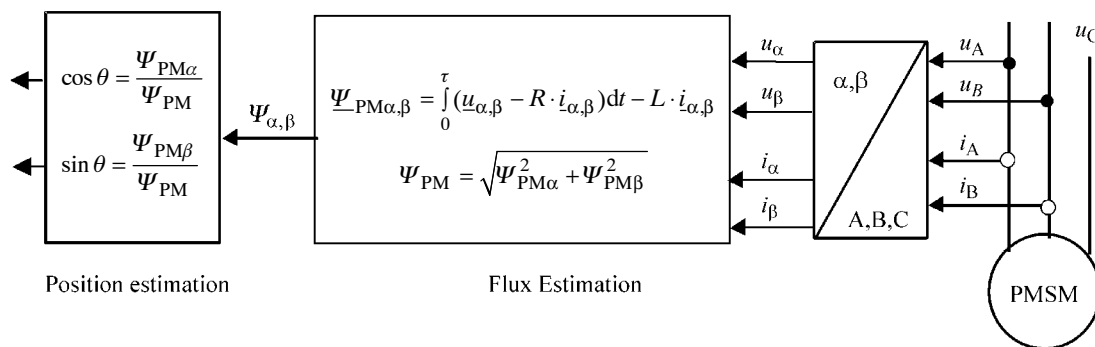


Fig. 7 A summarising diagram of direct flux estimating position estimator

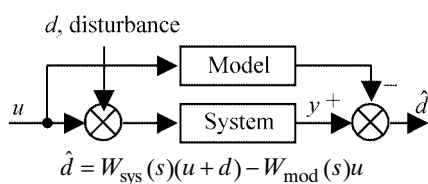


Fig. 8 Direct Model disturbance observer

re. This signal may be then low-pass filtered (LPF) in order to reduce the chattering in the observed signal. This algorithm is the simplest one and it is very useful.

Without the mathematical bases, the simplified observer implemented in our drive looks like (Figure 9).

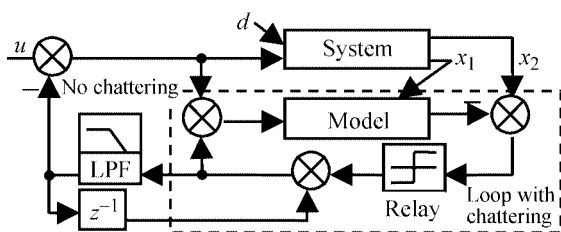


Fig. 9 Sliding mode disturbance compensation

Since LPF drastically decreases the speed of this controller, its time constant has been kept low. (Although our hardware is short circuit protected, and it has a hardware phase current limit in its MOSFET drivers, a fast current controller is really required for the vector controller to control the current vector.)

In vehicle application, a modified current control makes driveability better. At the start, a higher torque is required, while to achieve high speed the induced voltage needs to be reduced using field weakening. So d -direction current controlling is done. For optimum controlling of d -direction currents, see references [3, 4].

6 SLIDING-MODE SPEED AND TORQUE CONTROLLER WITHOUT ANY POSITION SENSOR [5]

This algorithm must be initialised with some starting algorithm studied before. This algorithm separately controls the d and q direction currents, in sliding mode (Figure 10). The model is one of the flux models studied above, in the rotor (d, q) or stator (α, β) reference frame. At first, it calculates the d and q direction torque-components, then it independently compensates them and uses hysteresis-relays to reduce the unwanted torque ripple and un-

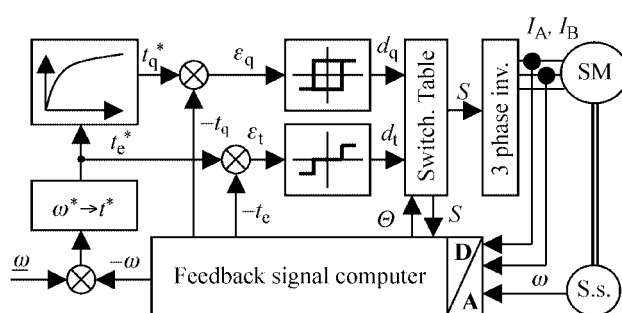


Fig. 10 The block diagram of the controller

predictable disturbances. From the status of the relays, the output switching signals are generated through a switching table. The output signals directly drive the switching devices of the three-phase inverter.

7 INITIALISATION

The common feature in these methods is that there are common unknowns required for operation. These are the electrical working parameters of the motor driven. These parameters must be defined or calculated before starting, otherwise these algorithms fail.

First of all, the current sensors are initialised through the measuring of their zero-current output. This is made by using a PI controller, so that accuracy is made high (in order to achieve high accuracy).

In the system first realised, the armature resistance and the armature inductivity are estimated by using the following method: using the current controller, a current vector in α direction is fed into the machine. The ratio of the terminal voltage and the current gives a resistance value, which is higher than the one measured with an ohmmeter due to the skin effect in the wire. In the next step, a low current, high speed (1 kHz) rotating field is generated. This cannot move the rotor, so the emf is negligible. From the motor model the inductivities $L_{d,q}$ and $|L|$ are calculated.

Starting is always done with the use of Hall-effect sensors. This is a »simple and good« method, having the advantage of its relative cheapness and high reliability. On the other hand, the accuracy of the direct flux estimation algorithm is directly proportional to the rotor speed and the induced voltage (our motors fail at about 10–20 % of the rated speed, depending on the effectiveness of the filtering of the current signals measured).

At the end of the starting procedure, the algorithm goes into closed loop synchronisation of the armature flux to the rotor flux. The best results so

far have been reached with a simple trick, namely that the effect of the field-oriented algorithm is weighed with the actual speed. So, at low speed, the rotor flux is commanded mainly by the Hall-effect sensors, while at higher speeds, where the accuracy of the field-oriented algorithm is good, it is highly applied.

8 NEURAL NETWORK BASED ON DTC

To improve the adaptability of an EV drive we have tried to build a neural network based on DTC control. The environment of this development was the SIMULINK subsystem of MATLAB.

The neural network of the motor model

Since only the phase currents and DC rail voltage are measured, the DTC controller must be based upon a motor model. Its main task is the as-accurate-as-possible determination of the stator flux amplitude and the torque of the motor.

Determination of the components of the stator flux

The inputs of the network are the DC rail voltage, the switching codes of the power transistors and the currents flowing in two phases. The neural network contains only one layer of two neurones whose activation functions are of SATLIN type. The flux vector is the integral of the difference of the phase voltage vector and the Ohmic-voltage drop vector. The required integrating feature is achieved by feeding back the neurones. The weighting factors of the neurones were set analytically. This structure and settings produce the flux components with satisfactory accuracy in any desirable situation.

The determination of flux and torque values

The determination of the motor torque and flux amplitude is the task of the neural network. For the torque estimation the flux and the current must be known. The flux amplitude can be determined from its Park-vector components. That is the reason why the flux vector components and the two phase currents were chosen as the inputs for the network. The fed-forward network of three layers being analysed is shown in Figure 11. This structure produced satisfactory accuracy of flux and torque estimation.

Switching table realisation in a neural network

In DTC, the torque and the stator flux amplitude are kept in a range around the command signal using two-point controllers. The voltage vector given on the machine depends on three factors: The stator flux amplitude error, the torque error and the

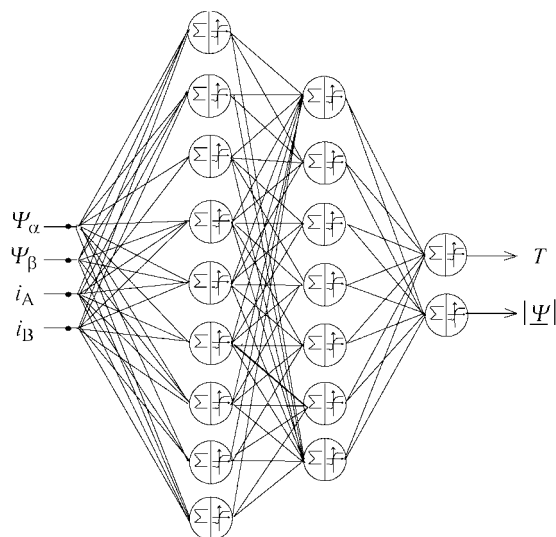


Fig. 11 Neural network of torque and flux estimation

direction of the flux vector. Since the torque and the flux controllers are relay controllers, they are realised with comparators. In the basic form of the DTC the comparator of the flux is of two-levels but experiences showed that in some cases it can not keep the flux amplitude in the range. The flux amplitude error can be reduced using a three-level comparator. The same result is obtained for the torque controller.

The switching table has got three inputs: the position code, the flux amplitude error code and the torque error code. The rotor position encoder of the PM synchronous machine is a similar 60-degree encoder commonly used in six-step EC motors.

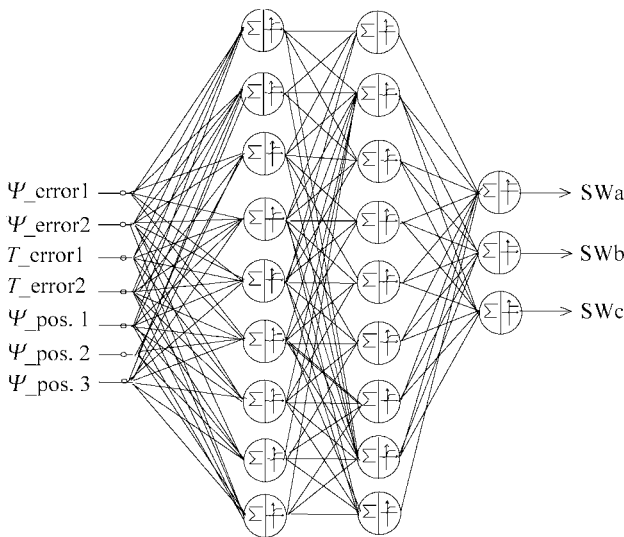


Fig. 12 Neural network of the switching table

Because of the initialisation of the third error level the originally 6×6 table was increased to 6×8 elements. The output codes of the switching table based on neural network means on (1) and off (0) states of the three upper transistors of the three alternating bridges (i.e. the lower transistors are switched oppositely to the upper ones). This table is represented in a 9-9-3 structured feed-forward type neural network (Figure 12). Unlike the common way of using HARDLIM functions in all the neurones, we used SIGMOID functions in the hidden layers and HARDLIM functions in the output layer. Our only reason for this is that more effective back-propagation training algorithms exist for the SIGMOID function. So the training time is shortened and the generalisation ability seems to be better than that of the HARDLIM-activated ones.

The simulation results of the DTC control based on neural network show that maybe this method will be very useful for driving an electrical vehicle.

9 EXPERIENCES WITH A WORKING SYSTEM

The tested system consists of PM synchronous motors for golf-cars, with a nearly sinusoidal emf shape and a reasonable L_d/L_q ratio of 1.3, a 12–36 V 100 A battery-voltage MOSFET inverter, and batteries. The

DSP software is written in C, for performance reasons.

The PC is a powerful means of software development for the DSP card. It offers editors, continuous debugging, data tracking, analysing and displaying tools for the DSP card. The following diagrams show the tracked data in the DSP in operation. It continuously displays any variables. In the diagrams, the input currents i_a , i_b , the main field fluxes Ψ_a , Ψ_b , the rotor flux $|\Psi_{PM}|$, rotor speed, actual torque and efficiency are shown in Figure 13.

We have created a development environment that consists of a PC with a DSP card, loading equipment with a measuring-controlling box and software for the PC.

Since all data are gathered in a single PC, all the required diagrams can be generated after a single measurement, which takes about a minute. In Figures 14–15 the typical characteristics of an EC drive measured by the computer controlled measurement system [1] are shown.

This integrated methodology of development and testing makes the longest part of the development process easier, faster and more suitable for documentation.

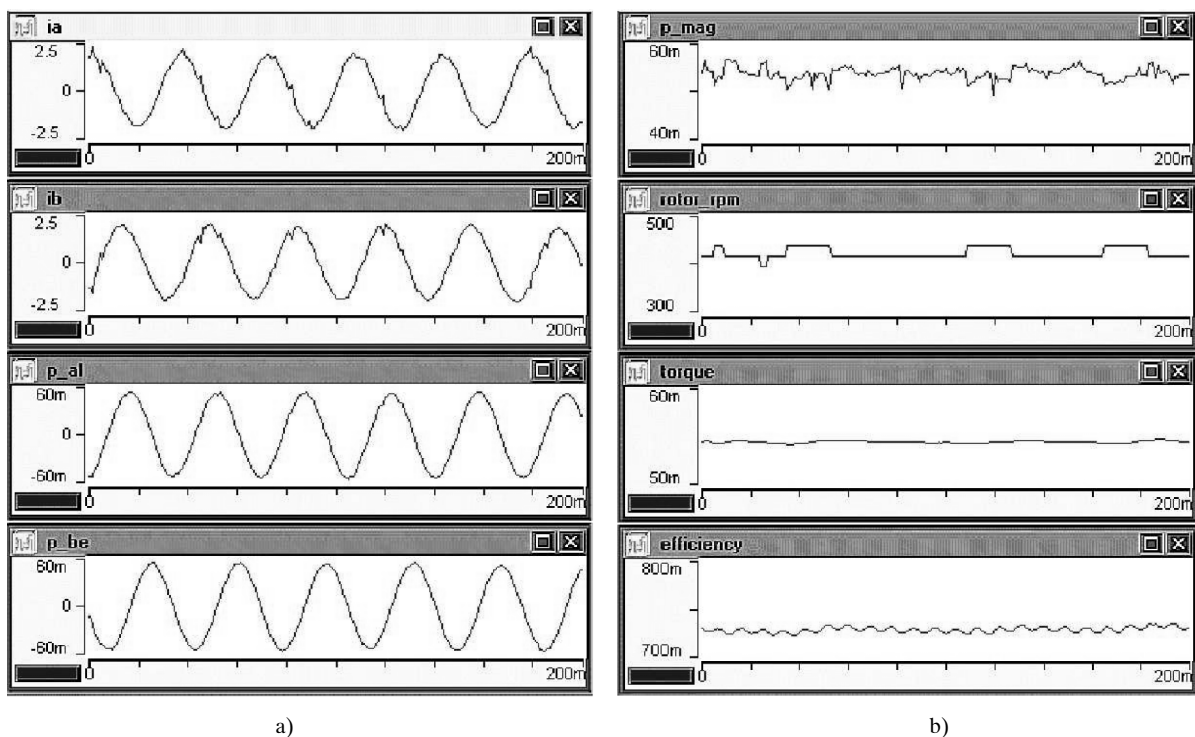
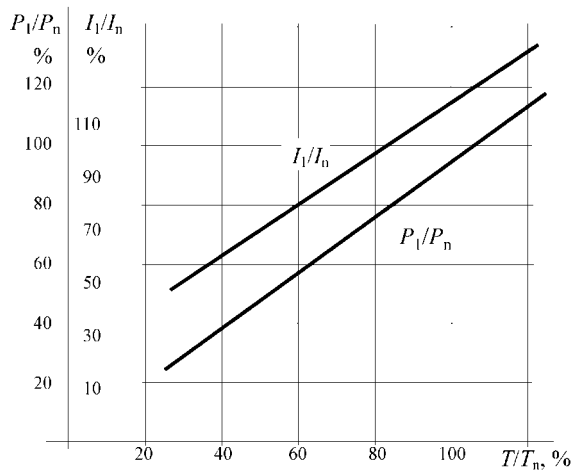


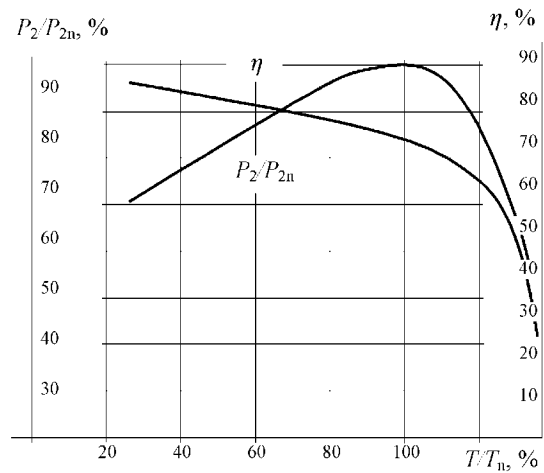
Fig. 13 Tracked data in DSP in operation: a) input currents and main field fluxes (no load current applied); b) observed rotor flux (unfiltered), rotor speed, torque and efficiency (no load current applied)

Load characteristics



a)

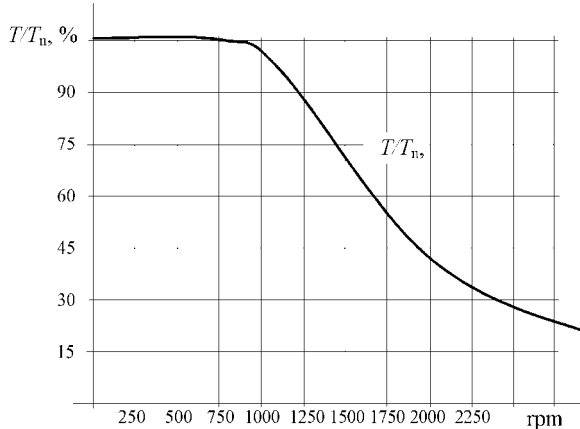
Load characteristics



b)

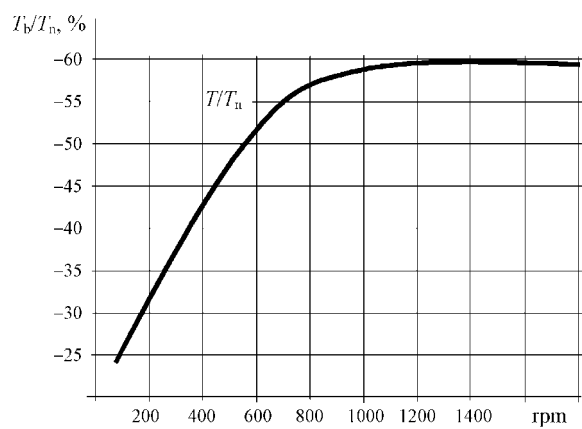
Fig. 14 Normalised load characteristics: a) $P(T)$ and $I(T)$; b) $P(T)$ and $\eta(T)$

Load characteristics



a)

Load characteristics



b)

Fig. 15 Torque – r.p.m. characteristics: a) in motor region b) in regenerative braking region

10 CONCLUSION

The opportunities in low power drive application of real-time controlling of PM brushless motors have drastically increased in recent years because high-performance DSP-s and power semiconductors have become easier to acquire and use than ever before. These devices are able to carry out complicated calculations so that real time model-based controlling techniques have rapidly spread.

DSP based system development can be carried out in an integrated system where the testing process can be automated, the measured and tracked

data can be matched together and continuously displayed, and characteristics can be drawn.

DSP-s are highly applicable in development, for simulating the final control system (even hardware) designed for a given application.

ACKNOWLEDGEMENT

The authors wish to thank the *JSPS Fellowship program*, *National Science Research Fund (OTKA T034654)* and *Control Research Group of Hungarian Academy of Science* for their financial support.

REFERENCES

- [1] Lóránt Nagy, Tibor Frank, **Microcomputer Controlled Measuring and Testing Equipment For Electric Machines**. Proceedings PEMC'96, vol. 2, pp. 532–536.
- [2] P. Korondi, K-K. David Young, Hideki Hashimoto: **Discrete-Time Sliding Mode Based Feedback Compensation for Motion Control**, Proceedings PEMC'96, vol 2, pp 244–248.
- [3] Morimoto, Takeda, Hirasa, Hatanaka, Tong, **Servo Drive System and Control Characteristics of a Salient Pole Permanent Magnet Synchronous Motor**, IEEE Transactions on Industry Applications, vol. 29, No. 2, March/April 1993.
- [4] Voltolini, Carlson, Sadowski, **Field Weakening of Brushless AC Drives: Motor Needed Characteristics and Control Strategy** 6, Proceedings PEMC'96, vol. 2, pp. 616–620.
- [5] Mihai Cernat, Peter Korondi, Vasile Comnac-Radu-Marian Cernat, **Sliding Mode Control of Interior Permanent Magnet Synchronous Motors**. Proceedings IPEC-Tokyo 2000, vol. 3, pp. 1116–1121.
- [6] Stephen J. Dodds, Jan Vittek, **Robust Position Control with Induction Motor**. Proceedings of EPE-PEMC2000 – 9th Power Electronics and Motion Control International Conference, Kosice, Slovak Republic, 5–7 September 2000, vol. 6, pp. 6–40.
- [7] Jan Vittek, Stephen J. Dodds, JuraJ Altus, Roy Perryman, **Sliding Mode Based Outer Control Loop for Sensorless Speed Control of Permanent Magnet Synchronous Motor**. Proceedings of the 8th IEEE Mediterranean Conference on Control and Automation (MED 2000) Rio, Patras, Greece, July 17–19, 2000.
- [8] Jan Vittek, Stephen J. Dodds, JuraJ Altus, Roy Perryman, **Vector Controlled Reluctance Synchronous Motor Drives with Prescribed Closed-Loop Dynamics**. Automatika, Journal for Control, Measurement, Electronics, Computing and Communications, KoREMA, Croatia, vol. 42. Y. 2001, No 1–2, pp. 29–36.
- [9] G. D. Andreescu, A. Popa, A. Spilca, **Two Sliding Mode Based Observers for Sensorless Control of PMSM**, Electro Pow Compo Sys 30(2), pp. 121–133, Feb 2002.
- [10] K. L. Shi, T. F. Chan, Y. K. Wong, S. L. Ho, **Direct Self Control of Induction Motor Based on Neural Network**, IEEE Transaction on Industry Application, vol. 37, No. 5, Sept. 2001.

Kompaktni motori i pogoni za električna vozila. S obzirom na veliku korisnost, beskolektorski motori s permanentnim magnetima na rotoru nalaze značajnu primjenu u električnim vozilima. U članku su opisani eksperimentalni rezultati razvoja beskolektorskih elektronički komutiranih motora integrirane izvedbe. Koriste se elektronički komutirani motori s pravokutnom strujom i trapezoidalnom idukcijom u zračnom rasporu kao i motori sa sinusoidalnom strujom i indukcijom, upravljani iz digitalnog signalnog procesora, (DSP). Razvijen je upravljački sustav s inverterom i motorom kao i upravljačka programska podrška. Analizirani su i simulacijski provjereni suvremeni algoritmi upravljanja te njihova primjenjivost na bilo koji tip navedenih motora.

Ključne riječi: električna vozila, beskolektorski pogoni, primjena u automobilskoj industriji, adaptivno upravljanje, digitalni signalni procesor (DSP), vektorsko upravljanje, neuronske mreže, klizni režim rada, simulacija

AUTHORS' ADDRESSES:

Gyula Knercz
 Budapest Polytechnic,
 Kandó Faculty of Electrical Engineering, Institute of Automation
 H-1034 Budapest 8, Pf. 112, Hungary
 +36-1-368-9893; knercz.gyula@kvk.bmf.hu

Lóránt Nagy
 Budapest Polytechnic,
 Kandó Faculty of Electrical Engineering, Institute of Automation
 H-1034 Budapest 8, Pf. 112, Hungary
 +36-1-368-9893; nagy.lorant@kvk.bmf.hu

Péter Korondi
 Budapest University of Technology and Economics
 Faculty of Electrical Engineering and Informatics
 Department of Automation and Applied Informatics
 H-1111 Budapest, Hungary
 +36-1-463-1165; korondi@elektro.get.bme.hu

Sándor Peresztegi
 Delco Remy Hungary Kft
 H-1034 Budapest 8, Pf. 112
 peresztegisandor@freemail.hu

Tamás Mezö
 WWINS Rt.
 H-1034 Budapest 8, Pf. 112
 tomfield@freemail.hu

Received: 2004–10–23